Journal of Cardiac Failure 32 (2026) 2034–2039

JCF
Journal of Cardiac Failure



Brief Report

AI-Enabled Opportunistic Splenic Phenotyping on Calcium-Scoring CT Identifies Residual Heart Failure Risk in Patients Without Coronary Calcium

ROHAN DHAMDHERE, MSc[1] SAMARTH MAHAPATRA[2] MENDEL LEBOWITZ, BS[1]
SANTOSH KUMAR SIRASAPALLI, MSc[3] SADEER AL-KINDI, MD[4] SANJAY RAJAGOPALAN, MD[5]
GOURAV MODANWAL, PhD[1,*] and ANANT MADABHUSHI, PhD[1,6,*]

Atlanta, GA; Berkeley, CA; Cleveland, OH; and Houston, TX

Key Words: Heart failure, spleen, radiomics, artificial intelligence.

Introduction

Preventing heart failure (HF) depends on identifying at-risk patients before symptoms develop, but existing tools remain imperfect. Coronary artery calcium (CAC) computerized tomography (CT), performed routinely for cardiovascular risk assessment, reliably reflects atherosclerotic risk but does not fully capture HF risk. A CAC score of 0 indicates no detectable atherosclerotic burden, yet these patients retain low but nonzero HF risk.[1,2] That residual risk is more often likely to be nonischemic, where atherosclerosis-oriented tools are least informative. The 2025 American Heart Association (AHA) primary-prevention statement frames this gap and highlights the need for additive biomarkers that reclassify PREVENT (Predicting Risk of Cardiovascular Disease EVENTs, an AHA online calculator)-calculated HF risk.[1]

Inflammation is increasingly implicated in HF pathogenesis, and the spleen is an emerging node in this process. In experimental models, myocardial injury mobilizes splenic immune cells that infiltrate the myocardium, propagating inflammation, fibrosis, and adverse remodeling through this cardiosplenic axis.[3–5] Within this axis, marrow-derived progenitors seed the spleen, where extramedullary hematopoiesis generates inflammatory myeloid cells implicated in HF with preserved ejection fraction (HFpEF).[6] Splenic metabolic activity on positron emission tomography predicts future cardiovascular events,[3] but it depends on specialized imaging ill-suited to population-scale screening. Alternatively, CAC CT captures the spleen on most scans, imaging an organ implicated in inflammatory HF.

Here we apply AI-derived radiomics to the opportunistically imaged spleen on CAC CT to derive an activated splenic imaging phenotype, hypothesizing that it is associated with incident HF. We test its independence from PREVENT risk and assess its incremental value in patients without detectable coronary calcium, where existing cardiovascular risk tools are weakest.

Methods

This retrospective single-center registry (NCT04075162), a no-charge community CAC screening program, comprised adults undergoing CAC CT on which the spleen was incidentally captured. Patients were excluded for pre-baseline HF, myocardial infarction, stroke, revascularization, or a non-HF cardiovascular event as the first post-baseline event. Spleens were segmented using a

From the [1]Wallace H. Coulter Department of Biomedical Engineering, Georgia Institute of Technology and Emory University, Atlanta, GA; [2]University of California, Berkeley, CA; [3]Department of Medicine, Case Western Reserve University, Cleveland, OH; [4]Center for CV Computational & Precision Health, Academy of Translational Research, Houston Methodist DeBakey Heart & Vascular Center, Houston Methodist, Houston, TX; [5]Department of Internal Medicine and Biomedical Engineering, University Hospitals Harrington Heart & Vascular Institute, Case Western Reserve University, Cleveland, OH and [6]Atlanta Veterans Affairs Medical Center, Atlanta, GA.

Manuscript received June 15, 2026; revised manuscript received August 13, 2026; revised manuscript accepted August 14, 2026.

Reprint requests: Anant Madabhushi, PhD, Wallace H. Coulter Department of Biomedical Engineering Georgia Institute of Technology and Emory University Health Sciences Research Building, 1750 Haygood Drive, Suite 647, Atlanta, GA 30322. E-mail: anantm@emory.edu

*Anant Madabhushi and Gourav Modanwal contributed equally as senior authors.

See page 2038 for disclosure information.

1071-9164/$ - see front matter

© 2026 The Author(s). Published by Elsevier Inc. This is an open access article under the CC BY-NC-ND license (http://creativecommons.org/licenses/by-nc-nd/4.0/)

https://doi.org/10.1016/j.cardfail.2026.08.015

previously validated deep-learning framework.[7] Incidental capture rendered only a small portion of the spleen, and masks below 500 voxels (~0.5–1.2 cm^3) were excluded as near-empty or failed segmentations (n = 762). The final cohort of 29,222 patients (mean age 59.4 ± 9.5 years; 50.0% male; 87.2% white, 7.5% Black; median follow-up 3.9 years, IQR 2.9-5.3) was split into a training set (n = 5844; 149 HF events) and a larger holdout set

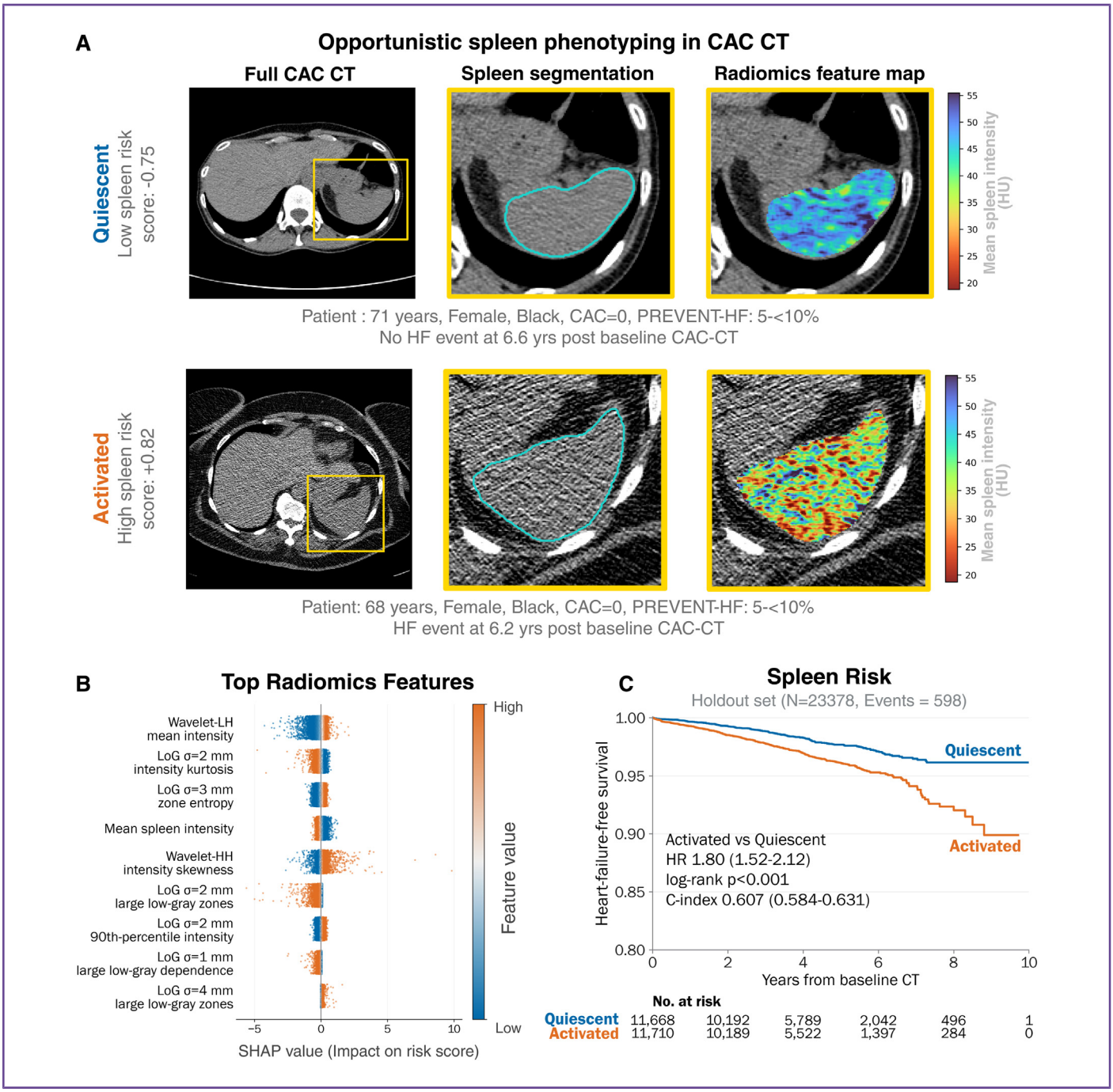


Fig. 1. Opportunistic CT radiomics identifies an activated splenic imaging phenotype that tracks incident heart failure. A, Representative quiescent (top) and activated (bottom) spleens on calcium-scoring CT, both with CAC = 0 and comparable PREVENT-HF risk. For each case, the full axial slice (left) shows the spleen incidentally captured on a routine scan, with the boxed region magnified to show the automated spleen segmentation outline (middle) and a voxel-level radiomic feature map (right, mean splenic attenuation). B, Radiomic features contributing to the spleen risk score, ranked by SHAP value. The score combines first-order intensity features (mean and 90th-percentile attenuation, skewness, kurtosis) and texture-heterogeneity features (zone entropy, large low-attenuation zones, large low-attenuation dependence), computed on the original image and after Laplacian-of-Gaussian and wavelet filtering. C, Holdout Kaplan-Meier by quiescent vs activated phenotype (training median), HR 1.80 (1.52–2.12), log-rank, $P < 0.001$. CAC, coronary artery calcium; CT computed tomography; HR, hazard ratio; PREVENT-HF, PREVENT (Predicting Risk of cardiovascular disease EVENTs) 10-year heart failure risk; SHAP, SHapley Additive exPlanations.

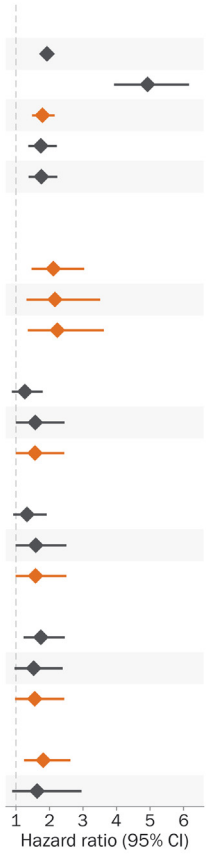
(n = 23,378; 598 HF events) reserved to power the prespecified analyses.

Radiomic features were extracted using PyRadiomics. In the training set, a LASSO-Cox model with 5-fold cross-validation selected 9 features (Fig. 1, B), combined into a spleen-risk score and applied unchanged to the holdout. Patients were dichotomized at the training-set median spleen-risk score (0.0863) into activated and quiescent phenotypes (Fig. 1, A). The binary phenotype was the primary exposure; the continuous per-standard deviation (SD) score was secondary.

The primary outcome was incident HF after baseline CAC-CT, with HFpEF and HF with reduced ejection fraction (HFrEF) subtypes ascertained from ICD-10 codes; non-HF deaths were treated as competing events (470 in the holdout).

Activated vs quiescent hazard ratios (HRs) were estimated in 3 nested models: unadjusted, adjusted for continuous PREVENT-HF 10-year risk (PREVENT-HF), and then, additionally, for race, the only standard risk factor it omits. Models were fit in the full holdout and within coronary-calcium strata to isolate residual HF risk. Independence from CAC and PREVENT-HF was quantified by Pearson correlation. Prespecified analyses tested spleen × CAC-stratum (CAC = 0 vs CAC >0) and HFpEF vs HFrEF interactions. Incremental discrimination was

Variable	HR (95% CI)	P-value	C-index (95% CI)	LR p	N	Events
Full holdout						
PREVENT-HF risk (per SD)	1.93 (1.81–2.05)	<0.001	0.740 (0.71–0.77)	—	11,888	368
PREVENT-HF ≥5%	4.93 (3.96–6.13)	<0.001	0.689 (0.66–0.71)	—	11,888	368
Spleen risk (unadjusted)	1.80 (1.52–2.12)	<0.001	0.607 (0.58–0.63)	—	23,378	598
adjusted for PREVENT-HF	1.75 (1.40–2.18)	<0.001	0.749 (0.72–0.78)	<0.001	11,888	368
adjusted for PREVENT-HF + race	1.77 (1.42–2.20)	<0.001	0.752 (0.72–0.78)	<0.001	11,888	368
CAC strata						
CAC = 0						
Spleen risk (unadjusted)	2.12 (1.50–3.00)	<0.001	0.608 (0.55–0.66)	—	9,798	135
adjusted for PREVENT-HF	2.17 (1.35–3.48)	0.001	0.696 (0.62–0.76)	0.002	4,911	75
adjusted for PREVENT-HF + race	2.24 (1.39–3.59)	<0.001	0.714 (0.65–0.77)	0.001	4,911	75
CAC 1–99						
Spleen risk (unadjusted)	1.27 (0.92–1.76)	0.15	0.571 (0.52–0.62)	—	7,019	146
adjusted for PREVENT-HF	1.58 (1.04–2.41)	0.034	0.712 (0.65–0.76)	0.019	3,506	94
adjusted for PREVENT-HF + race	1.58 (1.03–2.41)	0.035	0.711 (0.65–0.76)	0.019	3,506	94
CAC 100–399						
Spleen risk (unadjusted)	1.34 (0.95–1.88)	0.092	0.567 (0.51–0.62)	—	3,795	141
adjusted for PREVENT-HF	1.60 (1.03–2.47)	0.037	0.714 (0.66–0.78)	0.038	1,993	91
adjusted for PREVENT-HF + race	1.59 (1.03–2.47)	0.038	0.715 (0.65–0.78)	0.041	1,993	91
CAC ≥400						
Spleen risk (unadjusted)	1.75 (1.26–2.42)	<0.001	0.595 (0.55–0.64)	—	2,766	176
adjusted for PREVENT-HF	1.53 (1.00–2.36)	0.052	0.711 (0.66–0.76)	0.13	1,478	108
adjusted for PREVENT-HF + race	1.56 (1.01–2.41)	0.043	0.712 (0.66–0.76)	0.096	1,478	108
By HF subtype (ICD-10 defined)						
HFpEF	1.82 (1.28–2.59)	<0.001	0.788 (0.75–0.83)	0.002	11,888	148
HFrEF	1.64 (0.92–2.92)	0.093	0.772 (0.70–0.84)	0.052	11,888	53



- *HRs are for Activated vs Quiescent phenotype, except the two PREVENT-HF benchmark rows.*
- *Adjusted models use continuous PREVENT-HF (per SD); the ≥5% row is a threshold comparator; its HR is not comparable.*
- *Adjusted HRs are the Spleen association after listed adjustment.*
- *C-index and LR p use the continuous per-SD Spleen score.*
- *LR p tests whether adding Spleen improves the corresponding clinical model.*
- *Adjusted models are complete-case among patients with available PREVENT-HF data.*

Fig. 2. The activated splenic imaging phenotype is associated with incident HF, independent of clinical risk, consistently across coronary-calcium strata. Forest plot of activated-vs-quiescent hazard ratios (Cox proportional hazards, 95% CI). In the full holdout and within each of 4 coronary-calcium strata (0, 1−99, 100−399, ≥400 Agatston units), the phenotype is shown unadjusted, then adjusted for continuous PREVENT-HF 10-year risk, then additionally for race. The HFpEF and HFrEF rows use the PREVENT-HF- and race-adjusted model. Hazard ratios with *P* values are for the binary activated-vs-quiescent phenotype. The C-index (95% CI) and likelihood-ratio *P* reflect the continuous per-SD spleen score, with PREVENT-HF benchmarks shown per SD and at the ≥5% threshold. Threshold and per-SD hazard ratios are on different scales and are not directly comparable. Each row lists N and events. The 4-category spleen × CAC-stratum interaction was not significant ($P = 0.58$). Estimates were concordant under Fine-Gray competing-risk modeling. CAC, coronary artery calcium; C-index, concordance index; CI, confidence interval; HF, heart failure; HFpEF, HF with preserved ejection fraction; HFrEF, HF with reduced ejection fraction; HR, hazard ratio; PREVENT-HF, PREVENT (Predicting Risk of cardiovascular disease EVENTs) 10-year heart failure risk; SD, standard deviation; C-index, concordance index.

assessed by change in C index and likelihood-ratio tests. Within CAC = 0, restricted cubic splines modeled the continuous score for graded risk and nonlinearity, and joint stratification by phenotype and PREVENT-HF (<5% vs ≥5%) assessed risk separation, with Bonferroni sensitivity analysis for 6 pairwise comparisons. Robustness was assessed with cause-specific and Fine-Gray competing-risk models. Missing data were handled by complete-case analysis.

Results

In the holdout (n = 23,378; 598 events), the activated splenic phenotype was associated with lower HF-free survival than the quiescent phenotype (Fig. 1, C) (HR 1.80, 95% CI 1.52–2.12; log-rank, $P < 0.0001$), with risk rising continuously across the score (C-index 0.607, 0.584–0.631). The association was unchanged across stricter segmentation-size thresholds (HR 1.77–1.83, excluding up to 18%). It was independent of clinical risk, persisting after adjustment for PREVENT-HF and race (HR 1.77, 1.42–2.20; $P < 0.001$). The continuous score significantly improved discrimination over the clinical model (likelihood ratio $P < 0.001$) (Fig. 2). The score correlated weakly with CAC (r = 0.08) and PREVENT-HF (r = 0.12).

Adjusted for PREVENT-HF and race, the activated phenotype remained associated with HF across all 4 calcium strata: 2.24 (1.39–3.59; $P < 0.001$) at CAC = 0 (n = 9798; 135 events) and 1.56–1.59 (all $P < 0.05$) across the CAC >0 strata, without evidence of heterogeneity (4-category interaction; $P = 0.58$).

Within CAC = 0, the splenic phenotype refined PREVENT-HF-based risk. Modeled continuously, HF hazard rose steadily with no significant departure from linearity (per-SD HR 1.44, 1.27–1.63; $P < 0.001$; P for nonlinearity = 0.21), a dose-response rather than a single-threshold effect (Fig. 3, A). On joint stratification, risk rose stepwise across the 4 groups (P for trend <0.001) to HR 8.25 (4.28–15.91; $P < 0.001$) from PREVENT-low/Quiescent to PREVENT-elevated/Activated (Fig. 3, B). An activated spleen carried higher risk than a quiescent spleen within both PREVENT-HF groups, significantly among PREVENT-low patients (2.31, 1.27–4.21; $P = 0.006$) and directionally among PREVENT-elevated patients (2.02, 0.94–4.34; $P = 0.073$). And 5-year HF incidence rose from 0.8% to 5.7%. The association was significant for HFpEF (HR 1.82, 1.28–2.59; $P < 0.001$) but not for HFrEF (1.64, 0.92–2.92; $P = 0.09$), without a significant between-subtype difference (Fig. 2).

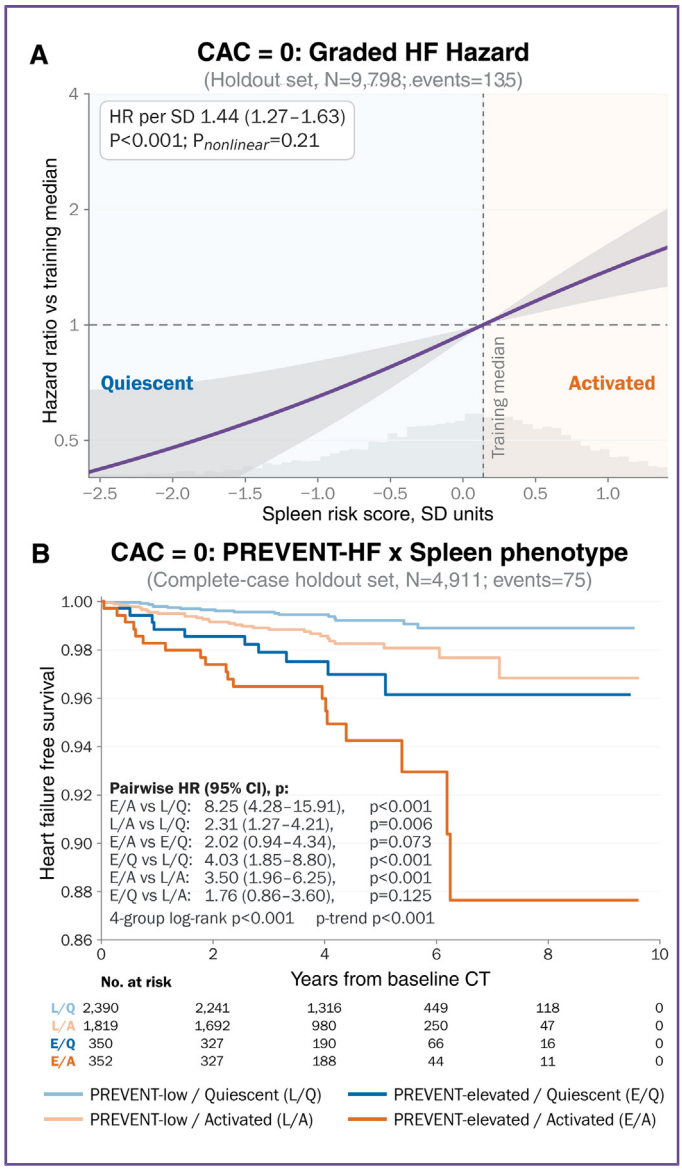


Fig. 3. In patients without coronary calcium, the splenic phenotype refines PREVENT-HF risk in a graded manner. A, CAC = 0 restricted cubic spline Cox model of HF hazard across the continuous spleen risk score, referenced to the training median (the Quiescent/Activated threshold). HF hazard rose continuously with no significant departure from linearity (P for nonlinearity = 0.21). The per-SD HR was 1.44 (1.27–1.63), and the C-index was 0.608 (0.55–0.66). B, CAC = 0 Kaplan-Meier by PREVENT-HF risk (PREVENT-low, <5%, vs PREVENT-elevated, ≥5%) and splenic phenotype (n = 4911, 75 events). Risk rose stepwise across the 4 groups (4-group log-rank, $P < 0.001$; Wald P for trend <0.001), reaching HR 8.25 (4.28–15.91; $P < 0.001$) from PREVENT-low/Quiescent to PREVENT-elevated/Activated. All 6 pairwise hazard ratios and nominal P values are shown; statistical significance was unchanged after Bonferroni correction. CAC, coronary artery calcium; C-index, concordance index; HF, heart failure; HR, hazard ratio; PREVENT-HF, PREVENT (Predicting Risk of cardiovascular disease EVENTs) 10-year heart failure risk; SD, standard deviation.

Discussion

An opportunistic splenic radiomic phenotype on CAC CT was associated with incident HF and remained informative, even without detectable coronary artery calcium levels, where atherosclerosis-based assessment is least informative. The association was independent of PREVENT-HF and race, graded across the continuous score and robust to competing-risk modeling and full clinical

adjustment. To our knowledge, this is among the first large-cohort studies to link a structural splenic phenotype to incident HF.

The phenotype is most useful clinically in patients with CAC = 0. Here it restratified risk significantly below the 5% PREVENT-HF threshold and directionally above it. This is biologically plausible; in experimental models, splenic immune-cell mobilization contributes to myocardial inflammation and fibrosis,[4,5] and splenic extramedullary hematopoiesis has been implicated in HFpEF.[6] Splenic intensity and textural heterogeneity plausibly reflect this splenic immune activation, consistent with prior radiogenomics.[8]

This study has limitations. It was single-center, and HF and subtype were ICD-10-ascertained, rendering the subtype and CAC = 0 analyses exploratory and reliant on modest event counts. Adjusted stratum estimates were complete-case, limited to the ~51% of patients with PREVENT-HF inputs, though the complete-case adjusted hazard closely matched the full-cohort unadjusted hazard. Incremental discrimination over PREVENT-HF was modest, the profile of an additive marker. HF biomarkers, echocardiography, histology, circulating immune markers, and fluorodeoxyglucose positron emission tomography (FDG-PET) were unavailable, precluding pre-HF ascertainment and leaving the cardiosplenic interpretation inferential; however, causal studies are needed.

No imaging biomarker predicts HF in isolation, and the spleen score is no exception. It modestly improves overall discrimination, so its value lies in the orthogonal information it adds; among CAC = 0 patients classified as low risk by PREVENT-HF, an activated spleen identified a subgroup with higher HF risk. Current primary-prevention guidance calls specifically for such an additive marker that refines PREVENT-based stratification rather than replacing it.[1] Obtained opportunistically from scans already acquired in routine care, it is a scalable candidate marker for nonatherosclerotic HF risk that warrants prospective and external validation.



Declaration of generative AI and AI-assisted technologies in the manuscript preparation process

During the preparation of this work, the authors used ChatGPT (OpenAI) and Claude (Anthropic) for manuscript organization, language editing, and formatting support. After using these tools, the authors reviewed and edited the content as needed and take full responsibility for the content of the published article.

Disclosures

AM is a Research Career Scientist at the Atlanta Veterans Affairs Medical Center and is an equity holder in Picture Health, Elucid Bioimaging, and Inspirata; he currently serves on the advisory board of Picture Health, consults for Takeda and Johnson & Johnson, and has sponsored research agreements with AstraZeneca and Bristol Myers-Squibb. His technology has been licensed to Picture Health and Elucid Bioimaging. RD, SM, ML, SKS, SA-K, SR, and GM report no conflicts of interest.

CRediT authorship contribution statement

ROHAN DHAMDHERE: Writing – review & editing, Writing – original draft, Visualization, Validation, Software, Methodology, Investigation, Formal analysis, Conceptualization. **SAMARTH MAHAPATRA:** Validation, Software. **MENDEL LEBOWITZ:** Writing – review & editing, Software. **SANTOSH KUMAR SIRASAPALLI:** Resources, Data curation. **SADEER AL-KINDI:** Supervision, Resources, Data curation, Conceptualization. **SANJAY RAJAGOPALAN:** Resources, Conceptualization. **GOURAV MODANWAL:** Writing – review & editing, Writing – original draft, Supervision, Software, Methodology, Investigation, Data curation, Conceptualization. **ANANT MADABHUSHI:** Writing – review & editing, Supervision, Resources, Methodology, Funding acquisition, Conceptualization.

Acknowledgments

Research reported in this publication was supported by the National Cancer Institute under award numbers R01CA249992-01A1, R01CA257612-01A1, R01CA264017-01, R01CA268287-01A1, U01CA113913-16A1, U01CA269181-01, U24CA274494-01; U54CA302465-01; R01CA268207-01; the National Heart, Lung and Blood Institute under award number R01HL158071-01A1; the National Institute of Allergy and Infectious Diseases under award numbers R01AI175555-01A1, and R01HL151277 01A1; the National Institute of Biomedical Imaging and Bioengineering under award number 75N92022D00015; the National Library of Medicine under award number R01LM013864-01A1; the National Institute on Aging under award number R01AG089759; the National Institute of Diabetes and Digestive and Kidney Diseases under award number R01DK118431; the Office of the Director, National Institutes of Health under award number 1OT2OD038065-01; the Kidney Mapping and Atlas Project (KMAP) under

award number U01DK133090-01; the United States Department of Veterans Affairs VA Merit Review under award number IBX004121; the VA Biomedical Laboratory Research and Development Service under award number IK6BX006185, the VA Research and Development Office through the Lung Precision Oncology Program LPOP-L0021; and by sponsored research agreements with Astrazeneca, Bristol Myers Squibb, the Prevent Cancer Foundation, Innovation in Cancer Informatics, the Institute for Technology in Health Care, the Breast Cancer Research Foundation, and the Scott R. Mackenzie Foundation. The content is solely the responsibility of the authors and does not necessarily represent the official views of the National Institutes of Health, the U.S. Department of Veterans Affairs, or the United States government. Figs.1, 2, and 3 were created in BioRender (Dhamdhere R. (2026) https://BioRender.com/xnq12rn.

References

1. Khan SS, Breathett K, Braun LT, et al. Risk-based primary prevention of heart failure: a scientific statement from the American Heart Association. Circulation 2025;151:e1006–26.
2. Hussain A, Ballantyne CM, Nambi V. Zero coronary artery calcium score: desirable, but enough? Circulation 2020;142:917–9.
3. Emami H, Singh P, MacNabb M, et al. Splenic metabolic activity predicts risk of future cardiovascular events: demonstration of a cardiosplenic axis in humans. JACC Cardiovasc Imag 2015;8:121–30.
4. Ismahil MA, Hamid T, Bansal SS, et al. Remodeling of the mononuclear phagocyte network underlies chronic inflammation and disease progression in heart failure. Circ Res 2014;114:266–82.
5. Prabhu SD. The cardiosplenic axis is essential for the pathogenesis of ischemic heart failure. Trans Am Clin Climatol Assoc 2018;129:202–14.
6. Hiraiwa H, Yura Y, Okumura T, Murohara T. Interplay of the heart, spleen, and bone marrow in heart failure: the role of splenic extramedullary hematopoiesis. Heart Fail Rev 2024;29:1049–63.
7. Modanwal G, Al-Kindi S, Walker J, et al. Deep-learning-based hepatic fat assessment (DeHFt) on non-contrast chest CT and its association with disease severity in COVID-19 infections: a multi-site retrospective study. EBioMed 2022;85:104315.
8. Kamineni M, Raghu V, Hua Z, et al. Machine learning–driven spleen imaging and genomics uncover a splenic connection to coronary artery disease. Sci Transl Med 2026;18:eaeh2517. https://doi.org/10.1126/scitranslmed.aeh2517.